PHYSICAL REVIEW D **78,** 083528 (2008)

Dark-energy dynamics required to solve the cosmic coincidence

Chas A. Egan*
Department of Astrophysics, School of Physics, University of New South Wales, Sydney, Australia

Charles H. Lineweaver+
Research School of Astronomy and Astrophysics, Australian National University, Canberra, Australia
(Received 26 December 2007; published 20 October 2008)

Dynamic dark-energy (DDE) models are often designed to solve the cosmic coincidence (why, just now, is the dark-energy density $\rho_{\rm de}$ the same order of magnitude as the matter density ρ_m?) by guaranteeing $\rho_{\rm de} \sim \rho_m$ for significant fractions of the age of the Universe. However, such behavior is neither sufficient nor necessary to solve the coincidence problem. Cosmological processes constrain the epochs during which observers can exist. Therefore, what must be shown is that a significant fraction of observers see $\rho_{\rm de} \sim \rho_m$. Precisely when, and for how long, must a DDE model have $\rho_{\rm de} \sim \rho_m$ in order to solve the coincidence? We explore the coincidence problem in dynamic dark-energy models using the temporal distribution of terrestrial-planet-bound observers. We find that any realistic DDE model which can be parametrized as $w = w_0 + w_a(1 - a)$ over a few e-folds has $\rho_{\rm de} \sim \rho_m$ for a significant fraction of observers in the Universe. This demotivates DDE models specifically designed to solve the coincidence using long or repeated periods of $\rho_{\rm de} \sim \rho_m$.

DOI: 10.1103/PhysRevD.78.083528 PACS numbers: 95.36.+x, 98.80.−k, 98.80.Es

I. INTRODUCTION

In 1998, using supernovae Ia as standard candles, Riess *et al.* [1] and Perlmutter *et al.* [2] revealed a recent and continuing epoch of cosmic acceleration—strong evidence that Einstein's cosmological constant Λ, or something else with comparable negative pressure $p_{\rm de} \sim -\rho_{\rm de}$, currently dominates the energy density of the Universe [3]. Λ is usually interpreted as the energy of zero-point quantum fluctuations in the vacuum [4,5] with a constant equation of state $w \equiv p_{\rm de}/\rho_{\rm de} = -1$. This necessary additional energy component, construed as Λ or otherwise, has become generically known as "dark energy" (DE).

A plethora of observations have been used to constrain the free parameters of the new standard cosmological model, ΛCDM, in which Λ *does* play the role of the dark energy. Hinshaw *et al.* [6] find that the Universe is expanding at a rate of $H_0 = 71 \pm 4$ km/s/Mpc; that it is spatially flat and therefore critically dense ($\Omega_{\rm tot0} = \frac{\rho_{\rm tot0}}{\rho_{\rm crit0}} = \frac{8\pi G}{3H_0^2}\rho_{\rm tot0} = 1.01 \pm 0.01$); and that the total density is comprised of contributions from vacuum energy ($\Omega_{\Lambda 0} = 0.74 \pm 0.02$), cold dark matter (CDM; $\Omega_{\rm CDM0} = 0.22 \pm 0.02$), baryonic matter ($\Omega_{b0} = 0.044 \pm 0.003$) and radiation ($\Omega_{r0} = 4.5 \pm 0.2 \times 10^{-5}$). Henceforth we will assume that the Universe is flat ($\Omega_{\rm tot0} = 1$) as predicted by inflation and supported by observations.

Two problems have been influential in moulding ideas about dark energy, specifically in driving interest in alternatives to ΛCDM. The first of these problems is concerned with the smallness of the dark-energy density [4,7,8]. Despite representing more than 70% of the total energy of the Universe, the current dark-energy density is ~120 orders of magnitude smaller than energy scales at the end of inflation (or ~80 orders of magnitude smaller than energy scales at the end of inflation if this occurred at the GUT rather than Planck scale) [7]. Dark-energy candidates are thus challenged to explain why the observed DE density is so small. The standard idea, that the dark energy is the energy of zero-point quantum fluctuations in the true vacuum, seems to offer no solution to this problem.

The second cosmological constant problem [9–11] is concerned with the near coincidence between the current cosmological matter density ($\rho_{m0} \approx 0.26 \times \rho_{\rm crit0}$) and the dark-energy density ($\rho_{\rm de0} \approx 0.74 \times \rho_{\rm crit0}$). In the standard ΛCDM model, the cosmological window during which these components have comparable density is short (just 105 e-folds of the cosmological scale factor a) since matter density dilutes as $\rho_m \propto a^{-3}$ while vacuum density $\rho_{\rm de}$ is constant [12]. Thus, even if one explains why the DE density is much less than the Planck density (the smallness problem), one must explain why we happen to live during the time when $\rho_{\rm de} \sim \rho_m$.

The likelihood of this coincidence depends on the range of times during which we suppose we might have lived. In works addressing the smallness problem, Weinberg [7,13,14] considered a multiverse consisting of a large number of big bangs, each with a different value of $\rho_{\rm de}$. There he asked, suppose that we could have arisen in any one of these universes; what value of $\rho_{\rm de}$ should we expect

*Visiting the Research School of Astronomy and Astrophysics, Australian National University.
chas@mso.anu.edu.au
+Also at Planetary Science Institute, Australian National University; Research School of Earth Sciences, Australian National University.

our Universe to have? While Weinberg supposed we could have arisen in another universe, we are simply supposing that we could have arisen in another time *in our Universe*. We ask, what time $t_{\rm obs}$, and corresponding densities $\rho_{\rm de}(t_{\rm obs})$ and $\rho_m(t_{\rm obs})$ should we expect to observe? Weinberg's key realization was that not every universe was equally probable: those with smaller $\rho_{\rm de}$ contain more Milky-Way-like galaxies and are therefore more hospitable [7,13]. Subsequently, he and other authors used the relative number of Milky-Way-like galaxies to estimate the distribution of observers as a function of $\rho_{\rm de}$, and determined that our value of $\rho_{\rm de}$ was indeed likely [15–17]. Our value of $\rho_{\rm de}$ could have been found to be unlikely and this would have ruled out the type of multiverse being considered. Here we apply analogous reasoning to the cosmic coincidence problem. Our observerhood could not have happened at any time with equal probability [12]. By estimating the temporal distribution of observers, we can determine whether the observation of $\rho_{\rm de} \sim \rho_m$ was likely. If we find $\rho_{\rm de} \sim \rho_m$ to be unlikely while considering a particular DE model, that will enable us to rule out that DE model.

In a previous paper [12], we tested ΛCDM in this way and found that $\rho_{\rm de} \sim \rho_m$ is expected. In the present paper we apply this test to dynamic dark-energy models to see what dynamics is required to solve the coincidence problem when the temporal distribution of observers is being considered.

The smallness of the dark-energy density has been anthropically explained in multiverse models with the argument that, in universes with much larger DE components, DE driven acceleration starts earlier and precludes the formation of galaxies and large scale structure. Such universes are probably devoid of observers [13,16,17]. A solution to the coincidence problem in this scenario was outlined by Garriga *et al.* [18], who showed that if $\rho_{\rm de}$ is low enough to allow galaxies to form, then observers in those galaxies will observe $r \sim 1$.

To quantify the time-dependent proximity of ρ_m and $\rho_{\rm de}$, we define a proximity parameter,

$$r \equiv \min\left[\frac{\rho_{\rm de}}{\rho_m}, \frac{\rho_m}{\rho_{\rm de}}\right], \tag{1}$$

which ranges from $r \approx 0$, when many orders of magnitude separate the two densities, to $r = 1$, when the two densities are equal. The presently observed value of this parameter is $r_0 = \frac{\rho_{m0}}{\rho_{\rm de0}} \approx 0.35$. In terms of r, the coincidence problem is as follows. If we naively presume that the time of our observation $t_{\rm obs}$ has been drawn from a distribution of times $P_t(t)$ spanning many decades of cosmic scale factor, we find that the expected proximity parameter is $r \approx 0 \ll 0.35$. In the top panel of Fig. 1 we use a naive distribution for $t_{\rm obs}$ that is constant in $\log(a)$ to illustrate how observing r as large as $r_0 \approx 0.35$ seems unexpected.

In Lineweaver and Egan [12] we showed how the apparent severity of the coincidence problem strongly depends upon the distribution $P_t(t)$ from which $t_{\rm obs}$ is hypothesized to have been drawn. Naive priors for $t_{\rm obs}$, such as the one illustrated in the top panel of Fig. 1, lead to naive conclusions. Following the reasoning of Weinberg [7,13,14], we interpret $P_t(t)$ as the temporal distribution of

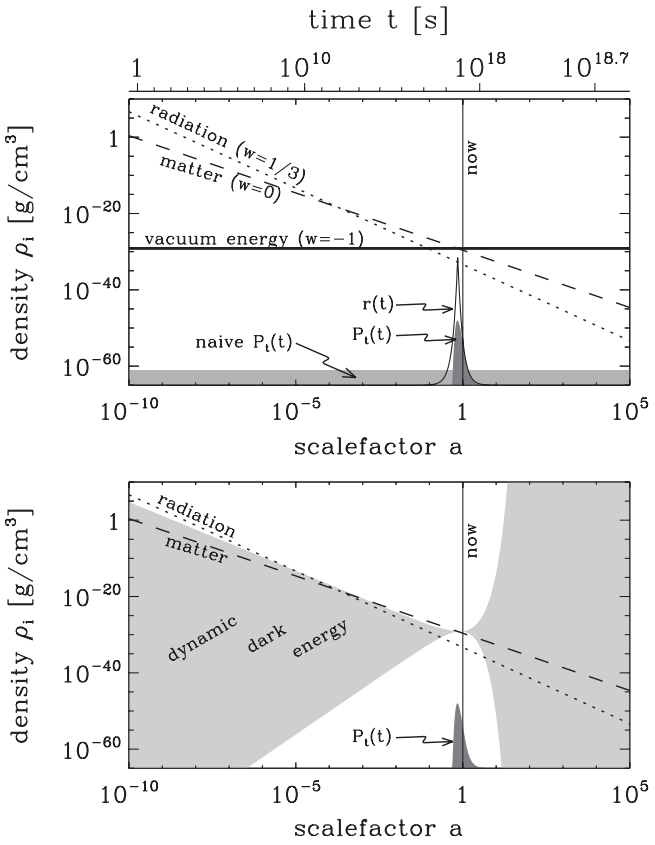

FIG. 1. (Top) The history of the energy density of the Universe according to standard ΛCDM. The dotted line shows the energy density in radiation (photons, neutrinos, and other relativistic modes). The radiation density dilutes as a^{-4} as the Universe expands. The dashed line shows the density in ordinary non-relativistic matter, which dilutes as a^{-3}. The thick solid line shows the energy of the vacuum (the cosmological constant) which has remained constant since the end of inflation. The thin solid peaked curve shows the proximity r of the matter density to the vacuum energy density [see Eq. (1)]. The proximity r is only $\sim$1 for a brief period in the $\log(a)$ history of the cosmos. Whether or not there is a coincidence problem depends on the distribution $P_t(t)$ for $t_{\rm obs}$. If one naively assumes that we could have observed any epoch with equal probability (the light gray shade) then we should not expect to observe r as large as we do. If, however, $P_t(t)$ is based on an estimate of the temporal distribution of observers (the dark gray shade) then $r_0 \approx 0.35$ is not surprising, and the coincidence problem is solved under ΛCDM [12]. (Bottom) The dark-energy density history is modified in DDE models. Observational constraints on the dark-energy density history are represented by the light gray shade (details in Sec. III).

observers. The temporal and spatial distribution of observers has been estimated using large ($10^{11} M_\odot$) galaxies [13,15,16,18] and terrestrial planets [12] as tracers. The top panel of Fig. 1 shows the temporal distribution of observers $P_t(t)$ from Lineweaver and Egan [12].

A possible extension of the concordance cosmological model that may explain the observed smallness of $\rho_{\rm de}$ is the generalization of dark-energy candidates to include dynamic dark-energy (DDE) models such as quintessence, phantom dark energy, k essence, and Chaplygin gas. In these models the dark energy is treated as a new matter field which is approximately homogenous, and evolves as the Universe expands. DDE evolution offers a mechanism for the decay of $\rho_{\rm de}(t)$ from the expected Planck scales (10^{93} g/cm^3) in the early Universe (10^{-44} s) to the small value we observe today (10^{-30} g/cm^3). The light gray shade in the bottom panel of Fig. 1 represents contemporary observational constraints on the DDE density history. Many DDE models are designed to solve the coincidence problem by having $\rho_{\rm de}(t) \sim \rho_m(t)$ for a large fraction of the history/future of the Universe [19–42]. With $\rho_{\rm de} \sim \rho_m$ for extended or repeated periods, the hope is to ensure that $r \sim 1$ is expected.

Our main goal in this paper is to take into account the temporal distribution of observers to determine when, and for how long, a DDE model must have $\rho_{\rm de} \sim \rho_m$ in order to solve the coincidence problem? Specifically, we extend the work of Lineweaver and Egan [12] to find out for which cosmologies (in addition to ΛCDM) the coincidence problem is solved when the temporal distribution of observers is considered. In doing this we answer the question: Does a dark-energy model fitting contemporary constraints on the density $\rho_{\rm de}$ and the equation of state parameters, necessarily solve the cosmic coincidence? Both positive and negative answers have interesting consequences. An answer in the affirmative will simplify considerations that go into DDE modeling: any DDE model in agreement with current cosmological constraints has $\rho_{\rm de} \sim \rho_m$ for a significant fraction of observers. An answer in the negative would yield a new opportunity to constrain the DE equation of state parameters *more strongly* than contemporary cosmological surveys.

A different coincidence problem arises when the time of observation is conditioned on and the parameters of a model are allowed to slide. The tuning of parameters and the necessity to include *ad hoc* physics are large problems for many current dark-energy models. This paper does not address such issues, and the interested reader is referred to Hebecker and Wetterich [43], Bludman [44], and Linder [45]. In the coincidence problem addressed here, we let the time of observation vary to see if $r(t_{\rm obs}) \geq 0.35$ is unlikely according to the model.

In Sec. II we present several examples of DDE models used to solve the coincidence problem. An overview of observational constraints on DDE is given in Sec. III. In Sec. IV we estimate the temporal distribution of observers. Our main analysis is presented in Sec. V. Our main result—that the coincidence problem is solved for all DDE models fitting observational constraints—is illustrated in Fig. 7. Finally, in Sec. VI, we end with a discussion of our results, their implications, and potential caveats.

II. DYNAMIC DARK-ENERGY MODELS IN THE FACE OF THE COSMIC COINCIDENCE

Though it is beyond the scope of this article to provide a complete review of DDE (see Copeland *et al.* [46],

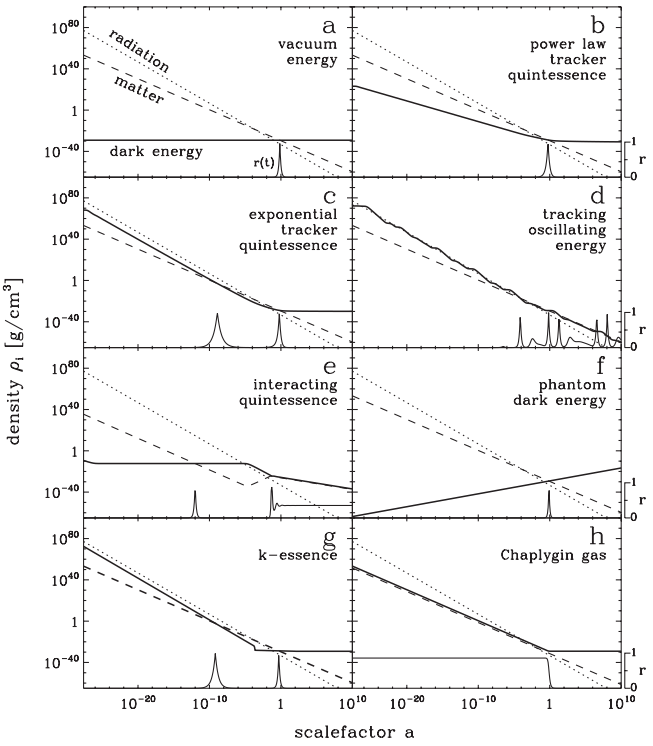

FIG. 2. The energy density history of the Universe according to ΛCDM [panel (a)], and seven DDE models selected from the literature (see text for references). In each panel the radiation and matter densities are the dotted and dashed lines, respectively. The DE density is given by the thick black line. The proximity parameter r is given by the thin black line at the base of each panel. Of the DDE models shown here, tracker quintessence and k essence [panels (b), (c), and (g)] have $r \sim 1$ for a small fraction of the life of the Universe (whether the abscissa is t, $\log(t)$, a, $\log(a)$, or any other of a large number of measures). On the other hand, tracking oscillating energy, interacting quintessence, phantom DE, and Chaplygin gas [panels (d), (e), (f), and (h)] exhibit $r \sim 1$ for a large fraction of the life of the Universe. For the phantom DE example [panel (f)] this is true in t, but not in a or $\log(a)$. In phantom models the future Universe grows super-exponentially to $a = \infty$ (a "big rip") shortly after matter-DE equality. Thus the Universe spends a large fraction of *time* with $r \sim 1$; however, this is not seen in $\log(a)$ space. For each of the models in this figure, numerical values for free parameters were chosen to crudely fit observational constraints and are given in the Appendix.

Szydłowski *et al.* [47]), here we give a few representative examples in order to set the context and motivation of our work. Figure 2 illustrates density histories typical of tracker quintessence, tracking oscillating energy, interacting quintessence, phantom dark energy, k essence, and Chaplygin gas. They are discussed in turn below.

A. Quintessence

In quintessence models, the dark energy is interpreted as a homogenous scalar field with Lagrangian density $\mathcal{L}(\phi, X) = \frac{1}{2}\dot{\phi}^2 - V(\phi)$ [48–54]. The evolution of the quintessence field and of the cosmos depends on the postulated potential $V(\phi)$ of the field and on any postulated interactions. In general, quintessence has a time-varying equation of state $w = \frac{p_{\rm de}}{\rho_{\rm de}} = \frac{\dot{\phi}^2/2 - V(\phi)}{\dot{\phi}^2/2 + V(\phi)}$. Since the kinetic term $\dot{\phi}^2/2$ cannot be negative, the equation of state is restricted to values $w \geq -1$. Moreover, if the potential $V(\phi)$ is non-negative then w is also restricted to values $w \leq +1$.

If the quintessence field only interacts gravitationally then energy density evolves as $\frac{\delta\rho_{\rm de}}{\rho_{\rm de}} = -3(w+1)\frac{\delta a}{a}$ and the restrictions $-1 \leq w \leq +1$ mean $\rho_{\rm de}$ decays (but never faster than a^{-6}) or remains constant (but never increases).

1. Tracker quintessence

Particular choices for $V(\phi)$ lead to interesting attractor solutions which can be exploited to make $\rho_{\rm de}$ scale (''track'') subdominantly with $\rho_r + \rho_m$.

The DE can be forced to transit to a Λ-like ($w \approx -1$) state at any time by fine-tuning $V(\phi)$. In the Λ-like state $\rho_{\rm de}$ overtakes ρ_m and dominates the recent and future energy density of the Universe. We illustrate tracker quintessence in Fig. 2 using a power law potential $V(\phi) = M\phi^{-\alpha}$ [panel (b)] [49,51,53] and an exponential potential $V(\phi) = M\exp(1/\phi)$ [panel (c)] [20].

The tracker paths are attractor solutions of the equations governing the evolution of the field. If the tracker quintessence field is initially endowed with a density off the tracker path (e.g. an equipartition of the energy available at reheating), its density quickly approaches and joins the tracker solution.

2. Oscillating dark energy

Dodelson *et al.* [20] explored a quintessence potential with oscillatory perturbations $V(\phi) = M\exp(-\lambda\phi) \times [1 + A\sin(\nu\phi)]$. They refer to models of this type as tracking oscillating energy. Without the perturbations (setting $A = 0$) this potential causes exact tracker behavior: the quintessence energy decays as $\rho_r + \rho_m$ and never dominates. With the perturbations the quintessence energy density oscillates about $\rho_r + \rho_m$ as it decays [Fig. 2(d)]. The quintessence energy dominates on multiple occasions and its equation of state varies continuously between positive and negative values. One of the main motivations for tracking oscillating energy is to solve the coincidence problem by ensuring that $\rho_{\rm de} \sim \rho_m$ or $\rho_{\rm de} \sim \rho_r$ at many times in the past or future.

It has yet to be seen how such a potential might arise from particle physics. Phenomenologically similar cosmologies have been discussed in Ahmed *et al.* [26], Feng *et al.* [37], and Yang and Wang [55].

3. Interacting quintessence

Nongravitational interactions between the quintessence field and matter fields might allow energy to transfer between these components. Such interactions are not forbidden by any known symmetry [56]. The primary motivation for the exploration of interacting dark-energy models is to solve the coincidence problem. In these models the present matter/dark-energy density proximity r may be constant [19,23,27,30–32,34,36,39–41,57] or slowly varying [29,35].

We plot a density history of the interacting quintessence model of Amendola [19] in Fig. 2(e). This model is characterized by a DE potential $V(\phi) = A\exp[B\phi]$ and DE-matter interaction term $Q = -C\rho_m\dot{\phi}$, specifying the rate at which energy is transferred to the matter fields. The free parameters were tuned such that radiation domination ends at $a = 10^{-5}$ and that $r_{t\to\infty} = 0.35$.

B. Phantom dark energy

The analyses of Riess *et al.* [58] and Wood-Vasey *et al.* [59] have mildly ($\sim 1\sigma$) favored a dark-energy equation of state $w_{\rm de} < -1$. These values are unattainable by standard quintessence models but can occur in phantom dark-energy models [60], in which kinetic energies are negative. The energy density in the phantom field *increases* with scale factor, typically leading to a future ''big-rip'' singularity where the scale factor becomes infinite in finite time. Figure 2(f) shows the density history of a simple phantom model with a constant equation of state $w = -1.25$. The big-rip ($a = \infty$ at $t = 57.5$ Gyrs) is not seen in $\log(a)$ space.

Caldwell *et al.* [61] and Scherrer [33] have explored how phantom models may solve the coincidence problem: since the big rip is triggered by the onset of DE domination, such cosmologies spend a significant fraction of their total time with r large. For the phantom model with $w = -1.25$ [Fig. 2(f)], Scherrer [33] finds $r > 0.1$ for 12% of the total lifetime of the Universe. Whether this solves the coincidence or not depends upon the prior probability distribution $P_t(t)$ for the time of observation. Caldwell *et al.* [61] and Scherrer [33] implicitly assume that the temporal distribution of observers is constant in time [i.e. $P_t(t) =$ constant]. For this prior the coincidence problem *is* solved because the chance of observing $r \geq 0.1$ is large (12%). Note that for the ''naive $P_t(t)$'' prior shown in Fig. 1, the solution of Caldwell *et al.* [61] and Scherrer [33] fails

because $r > 0.1$ is brief in $\log(a)$ space. It fails in this way for many other choices of $P_t(t)$ including, for example, distributions constant in a or $\log(t)$.

C. *k*-essence

In *k*-essence the DE is modeled as a scalar field with noncanonical kinetic energy [62–65]. Noncanonical kinetic terms can arise in the effective action of fields in string and supergravity theories. Figure 2(g) shows a density history typical of *k*-essence models. This particular model is from Armendariz-Picon *et al.* [64] and Steinhardt [11]. During radiation domination the *k*-essence field tracks radiation subdominantly (with $w_{\rm de} = w_r = 1/3$) as do some of the other models in Fig. 2. However, no stable tracker solution exists for $w_{\rm de} = w_m (= 0)$. Thus after radiation-matter equality, the field is unable to continue tracking the dominant component, and is driven to another attractor solution (which is generically Λ-like with $w_{\rm de} \approx -1$). The onset of DE domination was recent in *k*-essence models because matter-radiation equality prompts the transition to a Λ-like state. The *k*-essence thereby avoids fine-tuning in any particular numerical parameters, but the Lagrangian has been constructed *ad hoc*.

D. Chaplygin gas

A special fluid known as Chaplygin gas motivated by braneworld cosmology may be able to play the role of dark matter *and* the dark energy [66,67]. Generalized Chaplygin gas has the equation of state $p_{\rm de} = -A\rho_{\rm de}^{-\alpha}$ which behaves like pressureless dark matter at early times ($w_{\rm de} \approx 0$ when $\rho_{\rm de}$ is large), and like vacuum energy at late times ($w_{\rm de} \approx -1$ when $\rho_{\rm de}$ is small). In Fig. 2(h) we show an example with $\alpha = 1$.

E. Summary of DDE models

Two broad classes of DDE models emerge from our comparison:

(1) In ΛCDM, tracker quintessence and *k*-essence models, the dark-energy density is vastly different from the matter density for most of the lifetime of the Universe [panels (a), (b), (c), and (g) of Fig. 2]. The coincidence problem can only be solved if the probability distribution $P_t(t)$ for the time of observation is narrow, and overlaps significantly with an $r \sim 1$ peak. If $P_t(t)$ is wide, e.g. constant over the life of the Universe in t or $\log(t)$, then observing $r \sim 1$ would be unlikely in these models and the coincidence problem *is not* resolved.

(2) Tracking oscillating energy, interacting quintessence, phantom models, and Chaplygin gas models [panels (d), (e), (f), and (h) of Fig. 2] employ mechanisms to ensure that $r \sim 1$ for large fractions of the life of the Universe. In these models the coincidence problem may be solved for a wider range of $P_t(t)$ including, depending on the DE model, distributions that are constant over the whole life of the Universe in t, $\log(t)$, a, or $\log(a)$.

The importance of an estimate of the distribution $P_t(t)$ is highlighted: such an estimate will either rule out models of the first category because they do not solve the coincidence problem, or demotivate models of the second because their mechanisms are unnecessary to solve the coincidence problem. This analysis does not address the problems associated with fine-tuning, initial conditions, or ad hoc mechanisms of many DDE models [43–45].

We leave this line of enquiry temporarily to discuss contemporary *observational* constraints on the dark-energy density history, because we wish to test what DE dynamics are required to solve the coincidence, beyond those which models must exhibit to satisfy standard cosmological observations.

III. CURRENT OBSERVATIONAL CONSTRAINTS ON DYNAMIC DARK ENERGY

A. Supernovae Ia

Observationally, possible dark-energy dynamics is explored almost solely using measurements of the cosmic expansion history. Recent cosmic expansion is directly probed by using type Ia supernova (SNIa) as standard candles [1,2]. Each observed SNIa provides an independent measurement of the luminosity distance d_l to the redshift of the supernova $z_{\rm SN}$. The luminosity distance to $z_{\rm SN}$ is given by

$$d_l(z_{\rm SN}) = (1 + z_{\rm SN}) \frac{c}{H_0} \int_{z=0}^{z_{\rm SN}} \frac{dz}{E(z)}, \tag{2}$$

where

$$E(z) = \frac{H(z)}{H_0} = \left[\Omega_{r0}(1+z)^4 + \Omega_{m0}(1+z)^3 + \Omega_{\rm de0} \frac{\rho_{\rm de}(z)}{\rho_{\rm de0}} \right]^{1/2} \tag{3}$$

and thus depends on H_0, Ω_{m0}, and the evolution of the dark energy $\rho_{\rm de}(z)/\rho_{\rm de0}$. The radiation term, irrelevant at low redshifts, can be dropped from Eq. (3). $\Omega_{\rm de0}$ is a dependent parameter due to flatness ($\Omega_{\rm de0} = 1 - \Omega_{m0}$). Contemporary data sets include ~200 supernovae at redshifts $z_{\rm SN} \leq 2.16$ ($a \geq 0.316$) [59,68] and provide an effective continuum of constraints on the expansion history over that range [69,70]. The redshift range probed by SNIa is indicated in both panels of Fig. 3.

B. Cosmic microwave background

The first peak in the cosmic microwave background (CMB) temperature power spectrum corresponds to density fluctuations on the scale of the sound horizon at the

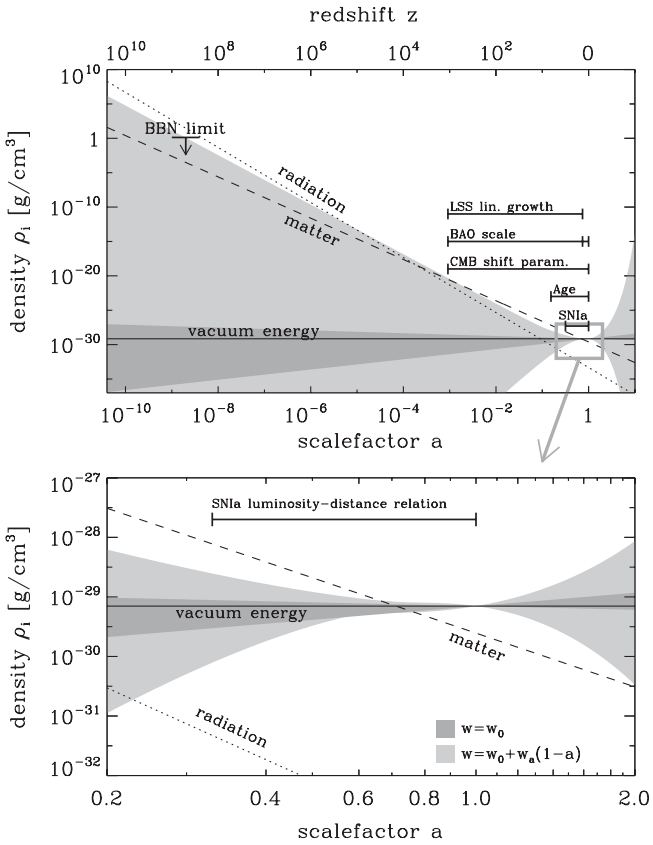

FIG. 3. The energy densities of radiation ρ_r, matter ρ_m, and the cosmological constant ρ_Λ are shown as a function of scale factor, by the dotted, dashed, and solid lines, respectively. Cosmological probes of dark energy include SNIa, CMB, BAO, the LSS linear growth factor and constraints from BBN (see text). Each of these probes is sensitive to the effects of dark energy over different redshift intervals, as indicated. The light gray band envelopes $w_0 - w_a$-parametrized DDE models allowed at $<2\sigma$ by Davis *et al.* [74] (the contour in $w_0 - w_a$ space is shown explicitly in Fig. 7). The dark gray band envelopes w_0-parametrized DDE models ($w_a = 0$ assumed) allowed at $<2\sigma$ by Wood-Vasey *et al.* [59]. The constraint is $w = -1.09 \pm 0.16$ at 2σ.

time of recombination. Subsequent peaks correspond to higher-frequency harmonics. The locations of these peaks in l space depend on the comoving scale of the sound horizon at recombination, and the angular distance to recombination. This is summarized by the so-called CMB shift parameter R [71,72] which is related to the cosmology by

$$R = \sqrt{\Omega_{m0}} \int_{z=0}^{z_{\rm rec}} \frac{dz}{E(z)}, \tag{4}$$

where $z_{\rm rec} \approx 1089$ [73] is the redshift of recombination. The three-year WMAP data gives a shift parameter $R = 1.71 \pm 0.03$ [73,74]. Since the dependence of Eq. (4) on H_0 and Ω_{m0} differs from that of Eq. (2), measurements of the CMB shift parameter can be used to break degeneracies between H_0, Ω_{m0} and DE evolution in the analysis of SNIa. In the top panel of Fig. 3 we represent the CMB observations using a bar from $z = 0$ to $z_{\rm rec}$.

C. Baryonic acoustic oscillations and large scale structure

As they imprinted acoustic peaks in the CMB, the baryonic oscillations at recombination were expected to leave signature wiggles—baryonic acoustic oscillations (BAO)—in the power spectrum of galaxies [75]. These were detected with significant confidence in the Sloan Digital Sky Survey (SDSS) luminous red galaxy power spectrum [76]. The expected BAO scale depends on the scale of the sound horizon at recombination, and on transverse and radial scales at the mean redshift $z_{\rm BAO}$, of galaxies in the survey. Eisenstein *et al.* [76] measured the quantity

$$A(z_{\rm BAO}) = \frac{\sqrt{\Omega_{m0}}}{E(z_{\rm BAO})^{1/3}} \left[\frac{1}{z_{\rm BAO}} \int_{z=0}^{z_{\rm BAO}} \frac{dz}{E(z)} \right]^{2/3} \tag{5}$$

to have a value $A(z_{\rm BAO} = 0.35) = 0.469 \pm 0.017$, thus constraining the matter density and the dark-energy evolution parameters in a configuration which is complementary to the CMB shift parameter and the SNIa luminosity distance relation. Ongoing BAO projects have been designed specifically to produce stronger constraints on the dark-energy equation of state parameter w. For example, WIGGLEZ [77] will use a sample of high-redshift galaxies to measure the BAO scale at $z_{\rm BAO} \approx 0.75$. As well as reducing the effects of nonlinear clustering, this redshift is at a larger angular distance, making the observed scale more sensitive to w. Constraints from the BAO scale depend on the evolution of the Universe from $z_{\rm rec}$ to $z_{\rm BAO}$ to set the physical scale of the oscillations. They also depend on the evolution of the Universe from $z_{\rm BAO}$ to $z = 0$, since the observed angular extent of the oscillations depends on this evolution. The bar representing BAO scale observations in the top panel of Fig. 3 indicates both these regimes.

The amplitude of the BAOs—the amplitude of the large scale structure (LSS) power spectrum—is determined by the amplitude of the power spectrum at recombination, and how much those fluctuations have grown (the transfer function) between $z_{\rm rec}$ and $z_{\rm BAO}$. By comparing the recombination power spectrum (from CMB) with the galaxy power spectrum, the LSS linear growth factor can be measured and used to constrain the expansion history of the Universe (independently of the BAO scale) over this redshift range. In practice, biases hinder precise normalization of the galaxy power spectrum, weakening this technique. The range over which this technique probes the DE is indicated in Fig. 3.

D. Ages

Cosmological parameters from SN1a, CMB, LSS, BAO, and other probes allow us to calculate the current age of the Universe to be 13.8 ± 0.1 [6] assuming ΛCDM. Uncertainties on the age calculated in this way grow dramatically if we drop the assumption that the DE is vacuum energy ($w = -1$).

An independent lower limit on the current age of the Universe is found by estimating the ages of the oldest known globular clusters [78]. These observations rule out models which predict the Universe to be younger than 12.7 ± 0.7 Gyrs (2σ confidence):

$$t_0 = H_0^{-1} \int_{z=0}^{\infty} \frac{dz}{(1+z)E(z)} \gtrsim 12.7 \pm 0.7 \text{ Gyrs}. \quad (6)$$

Other objects can also be used to set this age limit [79], but generally less successfully due to uncertainties in dating techniques.

Assuming ΛCDM, an age of 12.7 Gyrs corresponds to a redshift of $z \approx 5.5$. Contemporary age measurements are sensitive to the dark-energy content from $z \approx 5.5$ to $z = 0$. In the top panel of Fig. 3 we show this redshift interval. The evolution and energy content of the Universe before 12.7 Gyrs ago is not probed by these age constraints.

E. Nucleosynthesis

In addition to the constraints on the expansion history (SN1a, CMB, BAO, and t_0), we know that $\rho_{\rm de}/\rho_{\rm tot} < 0.045$ (at 2σ confidence) during big bang nucleosynthesis (BBN) [80]. Larger dark-energy densities imply a higher expansion rate at that epoch ($z \sim 6 \times 10^8$) which would result in a lower neutron to proton ratio, conflicting with the measured helium abundance, $Y_{\rm He}$.

F. Dark-energy parametrization

Because of the variety of proposed dark-energy models, it has become usual to summarize observations by constraining a parametrized time-varying equation of state. Dark-energy models are then confronted with observations in this parameter space. The unique zeroth order parametrization of w is $w = w_0$ (a constant), with $w = -1$ characterizing the cosmological constant model. The observational data can be used to constrain the first derivative of w. This additional dimension in the DE parameter space may be useful in distinguishing models which have the same w_0. From an observational standpoint, the obvious choice of 1st order parametrization is $w(z) = w_0 + \frac{dw}{dz} z$ [81]. This is rarely used today since currently considered DDE models are poorly portrayed by this functional form. The most popular parametrization is $w(a) = w_0 + w_a(1-a)$ [82,83], which does not diverge at high redshift.

Linder and Huterer [84] have argued that the extension of this approach to second order, e.g. $w(a) = w_0 + w_a(1-a) + w_{aa}(1-a)^2$, is not motivated by current DDE models. Moreover, they have shown that next generation observations are unlikely to be able to distinguish the quadratic from a linear expansion of w. Riess *et al.* [68] have illustrated this recently using new SN1a.

An alternative technique for exploring the history of dark energy is to constrain $w(z)$ or $\rho_{\rm de}(z)$ in independent redshift bins. This technique makes fewer assumptions about the specific shape of $w(z)$. In the absence of any strongly motivated parametrization of $w(z)$ this binwise method serves as a good reminder of how little we actually know from observation. Using luminosity distance measurements from SNIa, DE evolution has been constrained in this way in $\Delta z \sim 0.5$ bins out to redshift $z_{\rm SN} \sim 2$ [68,85,86]. In the future, BAO measurements at various redshifts may contribute to these constraints, however $z_{\rm BAO}$ will probably never be larger than $z_{\rm SN}$. Moreover, because the recombination redshift $z_{\rm rec} \approx 1089$ is fixed, only the cumulative effect (from $z = z_{\rm rec}$ to $z = 0$) of the DE can be measured with the CMB and LSS linear growth factor. With only this single data point above $z_{\rm SN}$, the binwise technique effectively degenerates to a parametrized analysis at $z > z_{\rm SN}$.

G. Summary of current DDE constraints

If one assumes the popular $w_0 - w_a$ parametrization until last scattering, then all cosmological probes can be combined to constrain w_0 and w_a. In a recent analysis of SN1a, CMB, and BAO observations, Davis *et al.* [74] found $w_0 = -1.0 \pm 0.4$ and $w_a = -0.4 \pm 1.8$ at 2σ confidence (the contour is shown in Fig. 7). Using the same observations, Wood-Vasey *et al.* [59] assumed $w_a = 0$ and found $w = w_0 = -1.09 \pm 0.16$ (2σ).

The evolution of $\rho_{\rm de}$ is related to w by covariant energy conservation [87]:

$$\frac{\delta\rho_{\rm de}}{\rho_{\rm de}} = -3(w(a)+1)\frac{\delta a}{a}. \quad (7)$$

The dark-energy density corresponding to the $w_0 - w_a$ parametrization of w is thus given by

$$\rho_{\rm de}(z) = \rho_{\rm de0} e^{3w_a(a-1)} a^{-3(1+w_0+w_a)}. \quad (8)$$

The cosmic energy density history is illustrated in Fig. 3. Radiation and matter densities steadily decline as the dotted and dashed lines. With the DE equation of state parametrized as $w(a) = w_0 + w_a(1-a)$, its density history is constrained to the light- gray area [74]. If the evolution of w is negligible, i.e. we condition on $w_a \approx 0$, then $w(a) \approx w_0$ and the DE density history lies within the dark- gray band [59]. If the dark energy is pure vacuum energy (or Einstein's cosmological constant) then $w = -1$ and its density history is given by the horizontal solid black line.

IV. THE TEMPORAL DISTRIBUTION OF OBSERVERS

The energy densities ρ_r, ρ_m, and $\rho_{\rm de}$, and the proximity parameter r we imagine we might have observed, depend on the distribution $P_t(t)$ from which we imagine our time of observation $t_{\rm obs}$ has been drawn. What we can expect to observe must be restricted by the conditions necessary for our presence as observers [88]. Thus, for example, it is meaningless to suppose we might have lived during inflation, or during radiation domination, or before the first atoms [89].

We can, however, suppose that we are randomly selected cosmology-discovering observers, and we can expect our observations of ρ_m and $\rho_{\rm de}$ to be typical of observations made by such observers. This is Vilenkin's principle of mediocrity [90]. Accordingly, the distribution $P_t(t)$ for the time of observation $t_{\rm obs}$ is proportional to the temporal distribution of cosmology-discovering observers (referred to henceforth as simply "observers"). Thus, to solve the coincidence problem one must show that the proximity parameter we measure, r_0, is typical of those measured by other observers.

The most abundant elements in the cosmos are hydrogen, helium, oxygen, and carbon [91]. In the past decade >200 extra solar planets have been observed via doppler, transit, or microlensing methods. Extrapolation of current patterns in planet mass and orbital period are consistent with the idea that planetary systems like our own are common in the Universe [92]. All this does not necessarily imply that observers are common, but it does support the idea that terrestrial-planet-bound carbon-based observers, even if rare, may be the *most common* observers. In the following estimation of $P_t(t)$, we consider only observers bound to terrestrial planets.

A. First the planets ...

Lineweaver [93] estimated the terrestrial planet formation rate (PFR) by making a compilation of measurements of the cosmic star formation rate (SFR) and suppressing a fraction of the early stars $f(t)$ to correct for the fact that the metallicity was too low for those early stars to host terrestrial planetary systems,

$$\mathrm{PFR}\,(t) = \mathrm{const} \times \mathrm{SFR}(t) \times f(t). \tag{9}$$

In Fig. 4 we plot the PFR reported by Lineweaver [93] as a function of redshift, $z = \frac{1}{a} - 1$. As illustrated in the figure, there is large uncertainty in the normalization of the formation history. The number of stars orbited by terrestrial planets normalizes the distribution of observers but, importantly, does not shift the distribution in time. Thus our analysis will not depend on the normalization of this function and this uncertainty *will not* propagate into our analysis. There are also uncertainties in the location of the turnover at high redshift, and in the slope of the formation history at low redshift—both of these *will* affect our results.

The conversion from redshift to time depends on the particular cosmology, through the Friedmann equation,

$$\left(\frac{da}{dt}\right)^2 = H(a)^2 a^2 = H_0^2[\Omega_{r0} a^{-2} + \Omega_{m0} a^{-1} + \Omega_{\rm de0} \exp[3w_a(a-1)] a^{-3w_0 - 3w_a - 1}]. \tag{10}$$

In Fig. 5 we plot the PFR from Fig. 4 as a function of time assuming the best-fit parametrized DDE cosmology.

B. ... then first observers

After a star has formed, some nontrivial amount of time $\Delta t_{\rm obs}$ will pass before observers, if they arise at all, arise on an orbiting rocky planet. This time allows planets to form and cool and, possibly, biogenesis and the emergence observers. $\Delta t_{\rm obs}$ is constrained to be shorter than the life of the host star. If we consider that our $\Delta t_{\rm obs}$ has been drawn from a probability distribution $P_{\Delta t_{\rm obs}}(t)$. The observer formation rate (OFR) would then be given by the convolution

$$\mathrm{OFR}\,(t) = \mathrm{const} \times \int_0^\infty \mathrm{PFR}(\tau) P_{\Delta t_{\rm obs}}(t-\tau) d\tau. \tag{11}$$

In practice we know very little about $P_{\Delta t_{\rm obs}}(t)$. It must be very nearly zero below about $\Delta t_{\rm obs} \sim 0.5$ Gyrs—this is the amount of time it takes for terrestrial planets to cool and the bombardment rate to slow down. Also, it is expected to be near zero above the lifetimes of sunlike stars (much above ~10 Gyrs). If we assume that our $\Delta t_{\rm obs}$ is typical, then $P_{\Delta t_{\rm obs}}(t)$ has significant weight around $\Delta t_{\rm obs} = 4$Gyrs—the amount of time it has taken for us to evolve here on Earth.

A fiducial choice, where *all* observers emerge 4 Gyrs after the formation of their host planet, is $P_{\Delta t_{\rm obs}}(t) = \delta(t - 4\ \mathrm{Gyrs})$. This choice results in an OFR whose shape is the

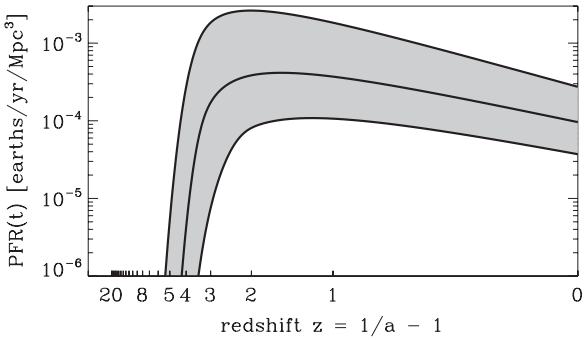

FIG. 4. The terrestrial planet formation rate as estimated by Lineweaver [93]. It is based on a compilation of SFR measurements and has been corrected for the low metallicity of the early Universe, which prevents the terrestrial planet formation rate from rising as quickly as the stellar formation rate at $z \gtrsim 4$.

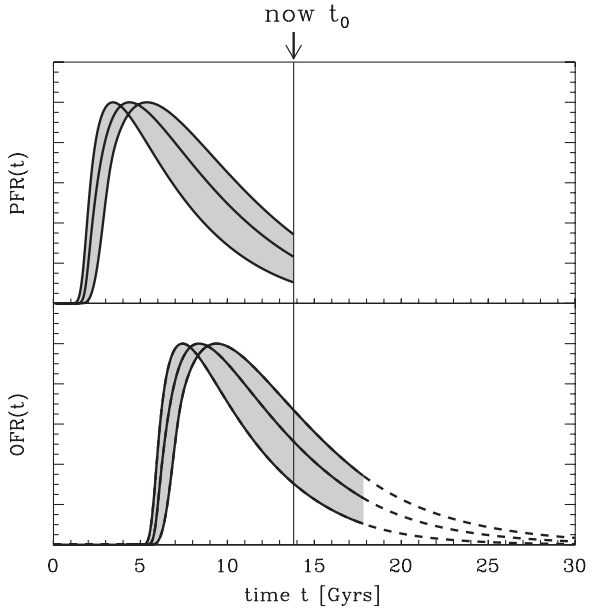

FIG. 5. The terrestrial planet formation from Fig. 4 is shown here as a function of time. The transformation from redshift to time is cosmology dependent. To create this figure we have used best-fit values for the DDE parameters, $w_0 = -1.0$ and $w_a = -0.4$ [74]. The y axis is linear (cf. the logarithmic axis in Fig. 4) and the family of curves have been renormalized to highlight the sources of uncertainty important for this analysis: uncertainty in the width of the function, and in the location of its peak. The observer formation rate (OFR) is calculated by shifting the planet formation rate by some amount $\Delta t_{\rm obs}$ ($= 4$ Gyrs) to allow the planet to cool, and the possible emergence of observers. These distributions are closed by extrapolating exponentially in t.

same as the PFR, but is shifted 4 Gyrs into the future,

$$\mathrm{OFR}\,(t) = \mathrm{const} \times \mathrm{PFR}(t - 4\ \mathrm{Gyrs}) \tag{12}$$

(see the lower panel of Fig. 5). Even for nonstandard w_0 and w_a values, this fiducial OFR aligns closely with the $r(t)$ peak and the effect of a wider $P_{\Delta t_{\rm obs}}$ is generally to increase the severity of the coincidence problem by spreading observers outside the $r(t)$ peak. Hence, using our fiducial $P_{\Delta t_{\rm obs}}$ (which is the narrowest possibility) will lead to conclusions which are conservative in that they underestimate the severity of the cosmic coincidence. If another choice for $P_{\Delta t_{\rm obs}}$ could be justified, the cosmic coincidence would be more severe than estimated here. We will discuss this choice in Sec. VI.

The OFR is then extrapolated into the future using a decaying exponential with respect to t (the dashed segment in the lower panel of Fig. 5). The observed SFR is consistent with a decaying exponential. We have tested other choices (linear and polynomial decay) and our results do not depend strongly on the shape of the extrapolating function used.

The temporal distribution of observers $P_t(t)$ is proportional to the observer formation rate,

$$P_t(t) = \mathrm{const} \times \mathrm{OFR}(t). \tag{13}$$

This observer distribution is similar to the one used by Garriga *et al.* [18] to treat the coincidence problem in a multiverse scenario. By comparison, our OFR(t) distribution starts later because we have considered the time required for the build up of metallicity, and because we have included an evolution stage of 4 Gyrs. Our distribution also decays more quickly than theirs does. Some of our cosmologies suffer big-rip singularities in the future. In these cases we truncate $P_t(t)$ at the big rip.

V. ANALYSIS AND RESULTS: DOES FITTING CONTEMPORARY CONSTRAINTS NECESSARILY SOLVE THE COSMIC COINCIDENCE?

For a given model the proximity parameter observed by a typical observer is described by a probability distribution $P_r(r)$ calculated as

$$P_r(r) = \sum \frac{dt}{dr} P_t(t(r)). \tag{14}$$

The summation is over contributions from all solutions of $t(r)$ (typically, any given value of r occurs at multiple times during the lifetime of the Universe). In Fig. 6 we plot $P_r(r)$ for the $w_0 = -1.0$, $w_a = -0.4$ cosmology. In this case, observers are distributed over a wide range of r values, with 71% seeing $r > r_0$, and 29% seeing $r < r_0$.

We define the severity S of the cosmic coincidence problem as the probability that a randomly selected observer measures a proximity parameter r lower than we do:

$$S = P(r < r_0) = 1 - P(r > r_0) = \int_{r=0}^{r_0} P_r(r) dr. \tag{15}$$

For the $w_0 = -1.0$, $w_a = -0.4$ cosmology of Figs. 5 and 6, the severity is $S = 0.29 \pm 0.09$. This model does not suffer a coincidence problem since 29% of observers would see r lower than we do. If the severity of the cosmic coincidence would be near 0.95 (0.997) in a particular model, then that model would suffer a 2σ (3σ) coincidence problem and the value of r we observe really would be unexpectedly high.

We calculated the severities S for cosmologies spanning a large region of the $w_0 - w_a$ plane and show our results in Fig. 7 using contours of equal S. The severity of the coincidence problem is low (e.g. $S \lesssim 0.7$) for most combinations of w_0 and w_a shown. There is a coincidence problem, where the severity is high ($S \gtrsim 0.8$), in two regions of this parameter space. These are indicated in Fig. 7.

Some features in Fig. 7 are worth noting:

(i) Dominating the left of the plot, the severity of the coincidence increases towards the bottom left-hand corner. This is because as w_0 and w_a become more

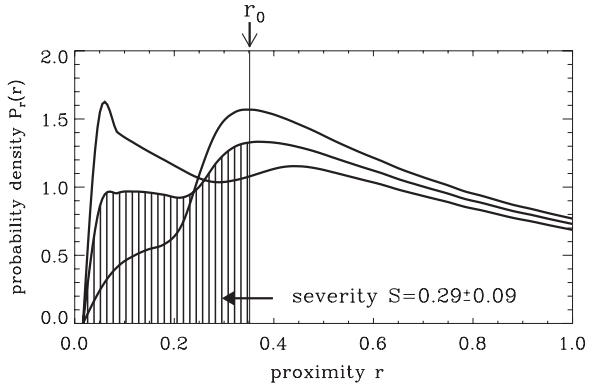

FIG. 6. The predicted distribution of observations of r is plotted for the parametrized DDE model which best fits cosmological observations: $w_0 = -1.0$ and $w_a = -0.4$. The proximity parameter we observe $r_0 = \frac{\rho_{m0}}{\rho_{de0}} \approx 0.35$ is typical in this cosmology since only 29% of observers (vertical striped area) observe $r < 0.35$. The upper and lower limits on this value resulting from uncertainties in the SFR are 38% and 20%, respectively. Thus the severity of the cosmic coincidence in this model is $S = 0.29 \pm 0.09$. This model does not suffer a coincidence problem.

negative, the r peak becomes narrower, and is observed by fewer observers.

(ii) There is a strong vertical dipole of coincidence severity centered at $(w_0 = 0,\ w_a = 0)$. For $(w_0 \approx 0,\ w_a > 0)$ there is a large coincidence problem because in such models we would be currently witnessing the very closest approach between DE and matter, with $\rho_{de} \gg \rho_m$ for all earlier and later times [see Fig. 8(c)]. For $(w_0 \approx 0,\ w_a < 0)$ there is an anticoincidence problem because in those models we would be currently witnessing the DDE's furthest excursion from the matter density, with ρ_{de} and ρ_m in closer proximity for all relevant earlier and later times, i.e., all times when $P_t(t)$ is non-negligible.

(iii) There is a discontinuity in the contours running along $w_a = 0$ for phantom models ($w_0 < -1$). The distribution $P_t(t)$ is truncated by big-rip singularities in strongly phantom models (provided they remain phantom; $w_a > 0$). This truncation of late-time observers means that early observers who witness large values of r represent a greater fraction of the total population.

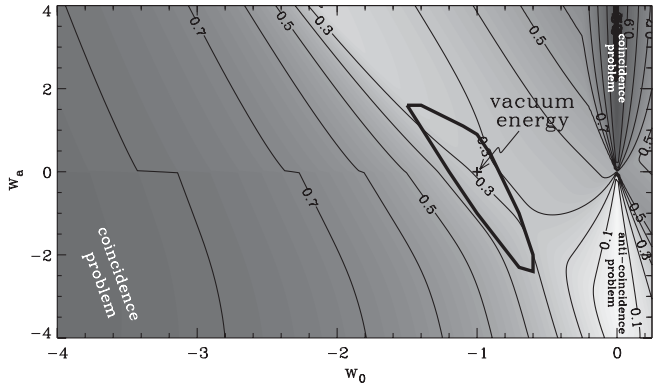

FIG. 7. Here we plot contours of equal severity S in $w_0 - w_a$ parameter space. S is the fraction of observers who see $r < r_0$. If S is large, a large percentage of observers should see r lower than we do—those models suffer coincidence problems. The thick black contour represents the observational constraints on w_0 and w_a from Davis *et al.* [74] (2σ confidence and marginalized over other uncertainties). In Lineweaver and Egan [12] we showed that the severity of the coincidence problem is low for ΛCDM (indicated by the "+"). Values of w_0 and w_a that result in a mild coincidence problem (e.g. $S \gtrsim 0.7$) are already strongly excluded by observations. This leads to our main result: none of the models in the observationally allowed regime suffer a cosmic coincidence problem when our estimate of the temporal distribution of observers $P_{obs}(t)$ is used as a selection function.

To illustrate these features, Fig. 8 shows the density histories and observer distributions for four specific examples selected from the $w_0 - w_a$ plane of Fig. 7.

We find that *all* observationally allowed combinations of w_0 and w_a result in low severities ($S < 0.4$), i.e., there are large ($> 60\%$) probabilities of observing the matter and vacuum density to be at least as close to each other as we observe them to be.

It is not suggested that for arbitrary models P_{obs} should be large when and only when $\rho_{de} \sim \rho_m$. Indeed, it is easy to imagine $\rho_{de} \sim \rho_m$ when there are not observers. Moreover, in some nonstandard cosmological models it is possible to contrive $\rho_{de} \ll \rho_m$ during times when observers do exist. What our results suggest is that, for models parametrized with w_0 and w_a satisfying current constraints, most observers ($> 60\%$) will see ρ_{de} and ρ_m nearly equal ($r > 0.35$).

VI. DISCUSSION

Particle-theoretic approaches to the cosmic coincidence problem have focused on the generation of a constant or slowly varying density ratio r. However, it has not been made clear precisely how slowly the ratio r must evolve in order to solve the coincidence problem. In other words, the question "What DDE dynamics are required to solve the coincidence problem?" has not been addressed.

In the present work we adopt the principle of mediocrity: that we should be typical observers, to try to answer this question. We estimate the temporal distribution of observers and devise a scheme for quantifying how unlikely the observation $r \geq 0.35$ is for an arbitrary DDE model. This scheme is applied to $w_0 - w_a$ parametric models, and we identify regions of the $w_0 - w_a$ parameter space in which the coincidence problem is most severe; however, these are already strongly excluded by observations (see Fig. 7).

Thus the main result of our analysis is that any realistic DDE model which can be parametrized as $w = w_0 + w_a(1 - a)$ over a few e-folds, has $\rho_{de} \sim \rho_m$ for a significant fraction of observers.

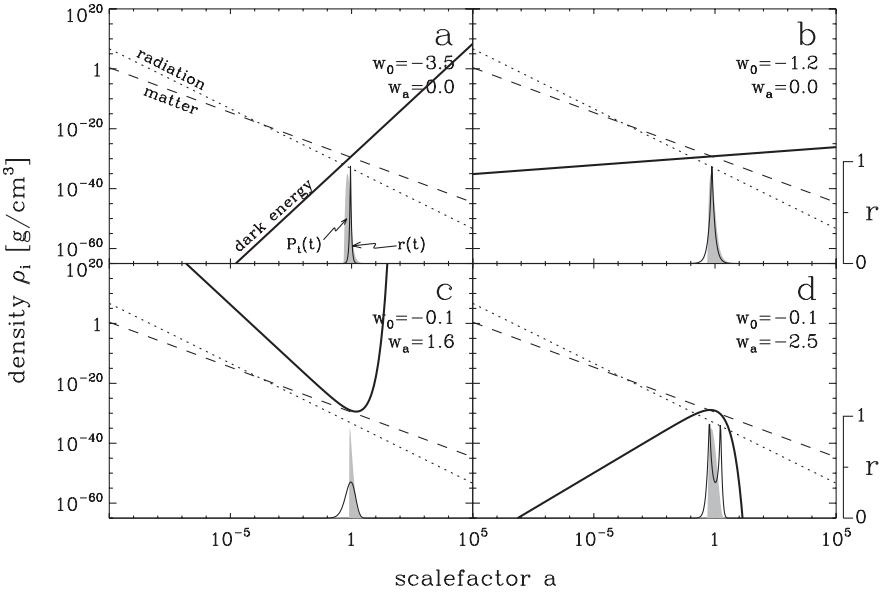

FIG. 8. History of the energy densities in radiation (dotted line), matter (dashed line), and dark energy (thick black line) for four parametrized DE models from Fig. 7. The proximity parameter r (thin black line) and the temporal distribution of observers $P_t(t)$ (gray shade) are also given. Panel (a) shows a phantom model with a constant equation of state $w = -3.5$. In this model the phantom density increases quickly and the $r(t)$ peak is narrow. As a result, a large fraction of observers live while the matter and dark-energy densities are vastly different ($r \approx 0$) and there is a mild coincidence problem ($S \approx 0.8$). This might be used to rule out the model shown in panel (a), except that it is already strongly excluded by direct cosmological observations (refer to Fig. 7). Panel (b) shows a phantom model which lies within the observationally allowed 2σ region. There is no coincidence problem in this model ($S \approx 0.4$). Panel (c) shows a model in which there is a coincidence problem ($S \approx 0.95$). This models lies within the cluster of contours in the upper right-hand corner of Fig. 7. In this model the dark energy dominates the past *and* future energy budget. Again however, the coincidence problem can tell us nothing new, as this model is already strongly excluded by observations. Panel (d) shows a model in which there is an anticoincidence problem. This models lies within the cluster of contours in the lower right-hand corner of Fig. 7. In this model the dark energy and matter densities are more similar (r is greater) in the recent past and near future (although $r \rightarrow 0$ further into the past or future). According to the observer distribution $P_t(t)$ most observers live near the current epoch, during $r > 0.35$, with just 7% living during $r < 0.35$ ($S = 0.07$) in this particular model. One might argue that this model can be ruled out because our value of r is anomalously small. However, this model too is already strongly excluded by observations.

Central to our approach is the temporal distribution of observers as estimated using the distribution of terrestrial planets. Such observer selection effects are operating. Thus, while they may be difficult to quantify, they need to be considered whenever the cosmic coincidence is used to motivate new physics. These anthropic considerations operate in conjunction with (not in place of) fundamental explanations of the dark energy.

Interacting quintessence models in which the proximity parameter asymptotes to a constant at late times [19,23,27,30–32,34,36,39–41,57] have been proposed as a solution to the coincidence problem. More recently, del Campo *et al.* [29,35] have argued for a broader class of interacting quintessence models that "soften" the coincidence problem by predicting a very slowly varying (though not constant) proximity parameter. Our analysis finds that r need not asymptote to a constant, nor evolve particularly slowly, partially undermining the motivations for these interacting quintessence models.

Caldwell *et al.* [61] and Scherrer [33] have proposed that the coincidence problem may be solved by phantom models in which there is a future big-rip singularity because such cosmologies spend a significant fraction of their lifetimes in $r \sim 1$ states. In our work $P_t(t)$ is terminated by big-rip singularities in ripping models. In nonripping models, however, the distribution is effectively terminated by the declining star formation rate. Therefore the big rip gives phantom models only a marginal advantage over other models. This marginal advantage manifests as the discontinuity along $w_a = 0$ on the left side of Fig. 7.

A running cosmological constant $\Lambda(t)$ could arise from the renormalization group (RG) in quantum field theory [94,95]. The running lambda term can mimic quintessence or phantom behavior and transit smoothly between the two [96]. RG models represent interesting alternatives to scalar-field models of dark energy. In some variants [97] additional fields are introduced to address the cosmic coincidence problem by predicting a slowly varying density ratio r. Our results demotivate such additions and favor simplistic RG models.

How strongly do these results depend on the assumed time it takes for observers to arise, $\Delta t_{\rm obs}$? In Lineweaver and Egan [12], where we performed an analysis similar to the present one (but limited to $w = -1$), we demonstrated

that the results were robust to any choice $\Delta t_{\rm obs} \sim [0, 11]$ Gyrs. However, for $\Delta t_{\rm obs} \gtrsim 12$ Gyrs that analysis resulted in an unavoidable coincidence problem because most observers would arise late (during DE domination) and would observe $\rho_{\rm de} \gg \rho_m$. The validity of the results of the present analysis are similarly limited.

We could improve our analysis, in the sense of getting tighter coincidence constraints (larger severities), if we used a less conservative $P_{\Delta t_{\rm obs}}$. We used the most conservative choice—a delta function—because the present understanding of the time it takes to evolve into observers is too poorly developed to motivate any other form of $P_{\Delta t_{\rm obs}}$. Another possible improvement is the DE equation of state parametrization. We used the current standard, $w = w_0 + w_a(1 - a)$, which may not parametrize some models well for very small or very large values of a.

We conclude that DDE models need not be fitted with exact tracking or oscillatory behaviors specifically to solve the coincidence by generating long or repeated periods of $\rho_{\rm de} \sim \rho_m$. Also, particular interactions guaranteeing $\rho_{\rm de} \sim \rho_m$ for long periods are not well motivated. Moreover, phantom models have no significant advantage over other DDE models with respect to the coincidence problem discussed here.

ACKNOWLEDGMENTS

C. E. acknowledges the UNSW School of Physics. C. E. thanks the ANU's RSAA for its kind hospitality, where this research was carried out.

TABLE . Free parameters of the DDE models illustrated in Fig. 2. These values were chosen such that observational constraints are crudely satisfied. These are by no means the only combinations fitting observations. These values are intended for the purposes of illustration in Fig. 2. Units are Planck units.

Model	Parameter	Value
Power law tracker quintessence	α	2
	M	1.4×10^{-124}
Exponential tracker quintessence	M	1.3×10^{-124}
Tracking oscillating energy	M	1.8×10^{-126}
	λ	4
	A	0.99
	ν	2.7
Interacting quintessence	A	1.4×10^{-119}
	B	9.7
	C	16
Chaplygin gas	α	1
	A	2.8×10^{-246}

APPENDIX: NUMERICAL VALUES FOR PARAMETERS OF MODELS ILLUSTRATED IN FIG. 2

In Fig. 2 we illustrate various DDE models from the literature. Values for the free parameters of these models were chosen such that the observational constraints are crudely satisfied. The values used are given in Table I. These are by no means the only combinations fitting observations.

[1] A. G. Riess *et al.*, Astron. J. **116**, 1009 (1998).
[2] S. Perlmutter *et al.*, Astrophys. J. **517**, 565 (1999).
[3] C. H. Lineweaver, Astrophys. J. **505**, L69 (1998).
[4] Y. B. Zel'Dovich, JETP Lett. **6**, 316 (1967).
[5] R. Durrer and R. Maartens, Gen. Relativ. Gravit. **40**, 301 (2008).
[6] G. Hinshaw, Legacy Archive for Microwave Background Data Analaysis (LAMBDA), http://lambda.gsfc.nasa.gov/product/map/current/params/lcdm_wmap_sdss.cfm.
[7] S. Weinberg, Rev. Mod. Phys. **61**, 1 (1989).
[8] J. D. Cohn, Astrophys. Space Sci. **259**, 213 (1998).
[9] S. Weinberg, arXiv:astro-ph/0005265.
[10] S. M. Carroll (SNAP (SuperNova Acceleration Probe) Collaboration), arXiv:astro-ph/0107571.
[11] P. J. Steinhardt, Proc. R. Soc. A **361**, 2497 (2003).
[12] C. H. Lineweaver and C. A. Egan, Astrophys. J. **671**, 853L (2007).
[13] S. Weinberg, Phys. Rev. Lett. **59**, 2607 (1987).
[14] S. Weinberg, Phys. Rev. D **61**, 103505 (2000).
[15] G. Efstathiou, Mon. Not. R. Astron. Soc. **274**, L73 (1995).
[16] H. Martel, P. R. Shapiro, and S. Weinberg, Astrophys. J. **492**, 29 (1998).
[17] L. Pogosian and A. Vilenkin, J. Cosmol. Astropart. Phys. 01 (2007) 025.
[18] J. Garriga, M. Livio, and A. Vilenkin, Phys. Rev. D **61**, 023503 (1999).
[19] L. Amendola, Phys. Rev. D **62**, 043511 (2000).
[20] S. Dodelson, M. Kaplinghat, and E. Stewart, Phys. Rev. Lett. **85**, 5276 (2000).
[21] V. Sahni and L. Wang, Phys. Rev. D **62**, 103517 (2000).
[22] L. P. Chimento, A. S. Jakubi, and D. Pavón, Phys. Rev. D **62**, 063508 (2000).
[23] W. Zimdahl, D. Pavón, and L. P. Chimento, Phys. Lett. B **521**, 133 (2001).
[24] V. Sahni, Classical Quantum Gravity **19**, 3435 (2002).
[25] L. P. Chimento, A. S. Jakubi, and D. Pavón, Phys. Rev. D **67**, 087302 (2003).
[26] M. Ahmed, S. Dodelson, P. B. Greene, and R. Sorkin, Phys. Rev. D **69**, 103523 (2004).
[27] U. França and R. Rosenfeld, Phys. Rev. D **69**, 063517 (2004).
[28] M. R. Mbonye, Mod. Phys. Lett. A **19**, 117 (2004).
[29] S. del Campo, R. Herrera, and D. Pavón, Phys. Rev. D **71**, 123529 (2005).

[30] Z.-K. Guo and Y.-Z. Zhang, Phys. Rev. D **71**, 023501 (2005).
[31] G. Olivares, F. Atrio-Barandela, and D. Pavón, Phys. Rev. D **71**, 063523 (2005).
[32] D. Pavón and W. Zimdahl, Phys. Lett. B **628**, 206 (2005).
[33] R. J. Scherrer, Phys. Rev. D **71**, 063519 (2005).
[34] X. Zhang, Mod. Phys. Lett. A **20**, 2575 (2005).
[35] S. del Campo, R. Herrera, G. Olivares, and D. Pavón, Phys. Rev. D **74**, 023501 (2006).
[36] U. França, Phys. Lett. B **641**, 351 (2006).
[37] B. Feng, M. Li, Y.-S. Piao, and X. Zhang, Phys. Lett. B **634**, 101 (2006).
[38] S. Nojiri and S. D. Odintsov, Phys. Lett. B **637**, 139 (2006).
[39] L. Amendola, M. Quartin, S. Tsujikawa, and I. Waga, Phys. Rev. D **74**, 023525 (2006).
[40] L. Amendola, G. C. Campos, and R. Rosenfeld, Phys. Rev. D **75**, 083506 (2007).
[41] G. Olivares, F. Atrio-Barandela, and D. Pavon, Phys. Rev. D **77**, 063513 (2008).
[42] G. Sassi and S. A. Bonometto, New Astron. Rev. **12**, 353 (2007).
[43] A. Hebecker and C. Wetterich, Phys. Lett. B **497**, 281 (2001).
[44] S. Bludman, Phys. Rev. D **69**, 122002 (2004).
[45] E. V. Linder, Phys. Rev. D **73**, 063010 (2006).
[46] E. J. Copeland, M. Sami, and S. Tsujikawa, Int. J. Mod. Phys. D **15**, 1753 (2006).
[47] M. Szydłowski, A. Kurek, and A. Krawiec, Phys. Lett. B **642**, 171 (2006).
[48] M. Özer and M. O. Taha, Nucl. Phys. **B287**, 776 (1987).
[49] B. Ratra and P. J. E. Peebles, Phys. Rev. D **37**, 3406 (1988).
[50] P. G. Ferreira and M. Joyce, Phys. Rev. D **58**, 023503 (1998).
[51] R. R. Caldwell, R. Dave, and P. J. Steinhardt, Phys. Rev. Lett. **80**, 1582 (1998).
[52] P. J. Steinhardt, L. Wang, and I. Zlatev, Phys. Rev. D **59**, 123504 (1999).
[53] I. Zlatev, L. Wang, and P. J. Steinhardt, Phys. Rev. Lett. **82**, 896 (1999).
[54] N. Dalal, K. Abazajian, E. Jenkins, and A. V. Manohar, Phys. Rev. Lett. **87**, 141302 (2001).
[55] G. Yang and A. Wang, Gen. Relativ. Gravit. **37**, 2201 (2005).
[56] L. Amendola, Mon. Not. R. Astron. Soc. **312**, 521 (2000).
[57] L. Amendola and C. Quercellini, Phys. Rev. D **68**, 023514 (2003).
[58] A. G. Riess *et al.*, Astrophys. J. **607**, 665 (2004).
[59] W. M. Wood-Vasey *et al.*, Astrophys. J. **666**, 694 (2007).
[60] R. R. Caldwell, Phys. Lett. B **545**, 23 (2002).
[61] R. R. Caldwell, M. Kamionkowski, and N. N. Weinberg, Phys. Rev. Lett. **91**, 071301 (2003).
[62] T. Chiba, T. Okabe, and M. Yamaguchi, Phys. Rev. D **62**, 023511 (2000).
[63] C. Armendariz-Picon, V. Mukhanov, and P. J. Steinhardt, Phys. Rev. Lett. **85**, 4438 (2000).
[64] C. Armendariz-Picon, V. Mukhanov, and P. J. Steinhardt, Phys. Rev. D **63**, 103510 (2001).
[65] M. Malquarti, E. J. Copeland, and A. R. Liddle, Phys. Rev. D **68**, 023512 (2003).
[66] M. C. Bento, O. Bertolami, and A. A. Sen, Phys. Rev. D **66**, 043507 (2002).
[67] A. Kamenshchik, U. Moschella, and V. Pasquier, Phys. Lett. B **511**, 265 (2001).
[68] A. G. Riess *et al.*, Astrophys. J. **659**, 98 (2007).
[69] Y. Wang and M. Tegmark, Phys. Rev. D **71**, 103513 (2005).
[70] Y. Wang and P. Mukherjee, Astrophys. J. **650**, 1 (2006).
[71] G. Efstathiou and J. R. Bond, Mon. Not. R. Astron. Soc. **304**, 75 (1999).
[72] O. Elgarøy and T. Multamäki, Astron. Astrophys. **471**, 65 (2007).
[73] D. N. Spergel *et al.*, Astrophys. J. Suppl. Ser. **170**, 377 (2007).
[74] T. M. Davis *et al.*, Astrophys. J. **666**, 716 (2007).
[75] D. J. Eisenstein and W. Hu, Astrophys. J. **496**, 605 (1998).
[76] D. J. Eisenstein *et al.*, Astrophys. J. **633**, 560 (2005).
[77] K. Glazebrook *et al.*, arXiv:astro-ph/0701876.
[78] B. M. S. Hansen, H. B. Richer, G. G. Fahlman, P. B. Stetson, J. Brewer, T. Currie, B. K. Gibson, R. Ibata, R. M. Rich, and M. M. Shara, Astrophys. J. Suppl. Ser. **155**, 551 (2004).
[79] C. H. Lineweaver, Science **284**, 1503 (1999).
[80] R. Bean, S. H. Hansen, and A. Melchiorri, Phys. Rev. D **64**, 103508 (2001).
[81] E. di Pietro and J.-F. Claeskens, Mon. Not. R. Astron. Soc. **341**, 1299 (2003).
[82] A. Albrecht *et al.*, arXiv:astro-ph/0609591.
[83] E. V. Linder, Astropart. Phys. **26**, 102 (2006).
[84] E. V. Linder and D. Huterer, Phys. Rev. D **72**, 043509 (2005).
[85] Y. Wang and M. Tegmark, Phys. Rev. Lett. **92**, 241302 (2004).
[86] D. Huterer and A. Cooray, Phys. Rev. D **71**, 023506 (2005).
[87] S. M. Carroll, *Spacetime and Geometry. An Introduction to General Relativity* (Addison-Wesley, San Francisco, CA, 2004), Vol. XIV, p. 513, ISBN 0-8053-8732-3.
[88] B. Carter, in *Confrontation of Cosmological Theories with Observational Data*, edited by M. S. Longair, IAU Symposium No. 63 (Reidel Publishing Company, Dordrecht, 1974), pp. 291–298.
[89] R. H. Dicke, Nature (London) **192**, 440 (1961).
[90] A. Vilenkin, Phys. Rev. Lett. **74**, 846 (1995).
[91] B. E. J. Pagel, in *Nucleosynthesis and Chemical Evolution of Galaxies* (Cambridge University Press, Cambridge, England, 1997), pp. 392, ISBN 0521550610.
[92] C. H. Lineweaver and D. Grether, Astrophys. J. **598**, 1350 (2003).
[93] C. H. Lineweaver, Icarus **151**, 307 (2001).
[94] I. L. Shapiro and J. Solà, Phys. Lett. B **475**, 236 (2000).
[95] A. Babić, B. Guberina, R. Horvat, and H. Štefančić, Phys. Rev. D **65**, 085002 (2002).
[96] J. Solà and H. Štefančić, Mod. Phys. Lett. A **21**, 479 (2006).
[97] J. Grande, J. Solà, and H. Štefančić, J. Cosmol. Astropart. Phys. 08 (2006) 011.